Progress In Electromagnetics Research Letters, Vol. 75, 83–89, 2018

Effect of Superstrate on a Cylindrical Microstrip Antenna

Prasanna K. Singh* **and Jasmine Saini**

Abstract—A microstrip patch antenna can be readily installed on any non-planar surface due to its conformal property, and this feature enhances its applicability in many areas. Moreover, in some specific applications, it is desirable and mandatory to provide protection of antenna from the unfriendly surroundings. Therefore, the present work focuses on the antenna with a dielectric cover and analyzes its effect on directivity, gain, and bandwidth at various superstrate air gaps. Two antenna models of single and dual elements are considered here separately, and both are conformal to the cylindrical surface. The antenna parameters are studied under varying superstrate gaps with equal intervals up to a quarter wavelength under fixed cylindrical curvature. It is noted that there is a significant improvement of 6% and 12% in bandwidth at quarter wavelength gap as compared to simple single and dual antenna models without dielectric loading, respectively. Also, both the calculated and measured results show the other important constructive effect of superstrate on the antenna performance.

1. INTRODUCTION

In many applications, patch antenna model is generally enclosed by a dielectric cover for protection and stealth purposes. The loading and bending of the dielectric superstrate affects the characteristics of a curved patch antenna profoundly [1–4]. The effectiveness of this dielectric cover can be enhanced further by satisfying the resonance condition which is at a quarter wavelength air gap from the antenna element. This paper attempts to examine the scope and usefulness of superstrate as an antenna performance tool. It should be noted that this technique is useful in minimizing the conventional antenna demerits such as narrow bandwidth and low gain with minimum cost and low design complexity. There are many papers which have analyzed antennas with dielectric loading on planar and non-planar surfaces using different approaches [5–9]. With the continuous advancement in technologies, the scope of enhancing the utilization of superstrate on antenna conformal to cylindrical surface can be devised. This dielectric superstrate causes significant effects on the characteristics of the microstrip antenna structure. It has been reported that a high gain can be achieved if the substrate and superstrate layers are used appropriately. The superstrate acts as a directive parasitic antenna, which considerably enhances the antenna gain. Dielectric cover layers have been used to enhance the directivity of antennas that are over a ground plane, based on the multiple-reflection phenomenon. Also, this type of dielectric overlay behaves as an aperture antenna, and it increases the effective aperture size which enhances the directivity beyond that of original antenna. The significant effect of dielectric coating on the antenna parameters are very well discussed and calculated [10, 11]. The theoretical formulations and observations are discussed in the subsequent sections.

2. MODEL FORMULATION

Consider a patch antenna mounted on an infinitely long cylinder-shaped surface of radius $\rho = R_1$ consisting of a PEC ground with a dielectric superstrate as depicted in Figure 1. Ideally, the patch

Received 28 February 2018, Accepted 9 April 2018, Scheduled 29 April 2018

* Corresponding author: Prasanna Kumar Singh (singhprasanna25@yahoo.com).
The authors are with the Department of Electronics and Communication Engineering, Jaypee Institute of Information Technology, A10, Sector-62, Noida-201307, Uttar Pradesh, India.

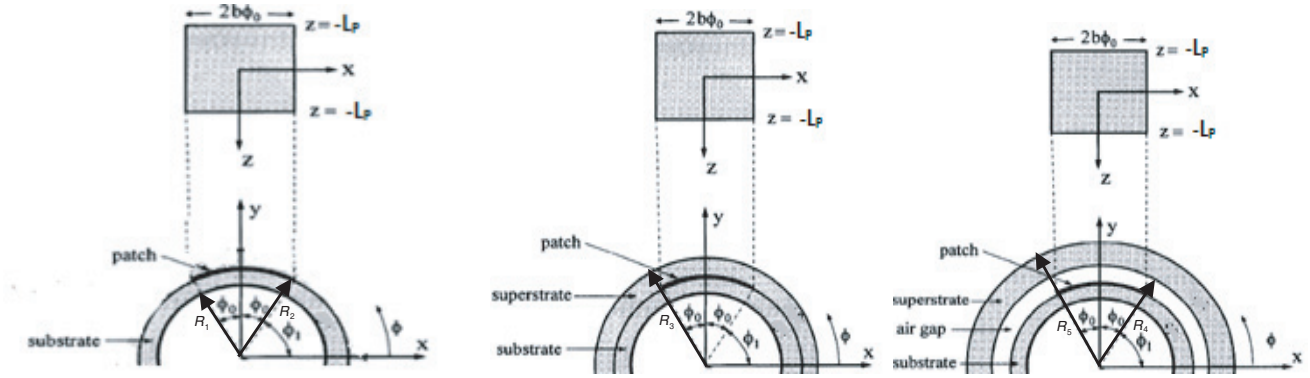

Figure 1. Geometric representations of patch antenna mounted on the cylindrical-shaped surface (a) without superstrate. (b) Flushed superstrate with no air gap, $N = 0$. (c) Air spaced superstrate with $N = 1$.

printed on the substrate is assumed to be PEC with minimal height ($\ll \lambda$) printed on the substrate. In this section, a rectangular patch with a dielectric superstrate is analyzed. The air gap, S_p, between the superstrate and patch can be gradually varied using the formula $S_p = N\lambda/4$, with $N = 0$, 0.25, 0.5, 0.75 and 1. The folded microstrip conformal to the cylinder-shaped surface is considered to have a straight length of $2L_p$ and a bent width W_P of $2b\phi_0$. The theoretical formulation of the antenna model is divided into four sectors depending upon the physical condition and field components. Figure 1 shows the three geometric configurations of the antenna model w.r.t. no loading, loading with no spacing, and air spacing loading, respectively. Consider the case of Figure 1(a), where the boundary condition is applied at $\rho = R_2$. In the second case as shown in Figure 1(b), the antenna is flushed mounted on the superstrate. The boundary conditions are therefore applied at $\rho = R_2$ and R_3. Finally, in the last case as depicted in Figure 1 (c), the antenna model is covered by air spaced dielectric loading, and the boundary condition is applied at $\rho = R_4$ and R_5. The cylindrical substrate with radius $\rho = R_2$ has a relative permittivity ε_{r1} represented as Section 1 (in Figure 1(a)), with thickness of $R_1 < \rho < R_2$. The free air space region $\rho > R_2$ designated as Section 2 (in Figure 1(b)) above the antenna has a permittivity ε_0. The antenna when being loaded with a dielectric at radius $\rho = R_3$ is designated as Section 3 (in Figure 1(c)) and has a thickness of $R_2 < \rho < R_3$ and relative permittivity ε_{r1}. Now, an alike cylindrical superstrate with a thickness of $R_4 < \rho < R_5$ is spaced off up to $R_2 < \rho < R_4$ air gap with the region denoted as Section 4. The outermost area $\rho > R_5$ is the free air space with permittivity ε_0 designated as Section 5. Initially, the field components in the respective sectors (where the media is changing) are determined by applying the boundary conditions at various sectors for the tangential electric and magnetic fields. Assuming a time harmonic dependence of $(-e^{j\omega t})$, the z components of the electric and magnetic fields in the qth sector for $q = 1, 2, 3, 4$ can be expressed in a cylindrical coordinate system (ρ, ϕ, z) as [1, 5, 9]

$$E_{qz}(\rho,\phi,z) = \frac{1}{2\pi}\sum_{n=-\infty}^{\infty} e^{jn\phi}\int_{-\infty}^{\infty} dk_z e^{jk_z z}[A_{qn}H_n^{(2)}(k_{q\rho}\rho) + B_{qn}J_n(k_{q\rho}\rho)] \tag{1}$$

$$H_{qz}(\rho,\phi,z) = \frac{1}{2\pi}\sum_{n=-\infty}^{\infty} e^{jn\phi}\int_{-\infty}^{\infty} dk_z e^{jk_z z}[C_{qn}H_n^{(2)}(k_{q\rho}\rho) + D_{qn}J_n(k_{q\rho}\rho)] \tag{2}$$

where k_z is the propagation constant, $k_{q\rho}^2 = \omega^2\mu_0\varepsilon_q - k_z^2$, $\varepsilon_q = \varepsilon_0\varepsilon_{rq}$; A_{qn}, B_{qn}, C_{qn}, D_{qn} are the unknown expansion coefficients of harmonic order n to be determined by the boundary conditions at respective sectors and are functions of k_z. $J_n(x)$ and $H_n^{(2)}(x)$ are the Bessel function and second kind Hankel function of order n and argument x, respectively. The tangential electric field components on the antenna can be found and are related to the surface current density of patch. Finally, a set of the

vector integral equations can be found by applying all boundary conditions on the rectangular microstrip antenna and outside the rectangular microstrip antenna at $\rho = R_2$, that is,

On the rectangular microstrip antenna,

$$\begin{bmatrix} E_\phi(\phi,z) \\ E_z(\phi,z) \end{bmatrix} = \frac{1}{2\pi}\sum_{n=-\infty}^{\infty} e^{jn\phi}\int_{-\infty}^{\infty} dk_z e^{jk_z z}\overset{\cong}{X}(n,k_z)\begin{bmatrix} \tilde{J}_{\phi n}(k_z) \\ \tilde{J}_{zn}(k_z) \end{bmatrix} = \begin{bmatrix} 0 \\ 0 \end{bmatrix} \tag{3}$$

and outside the rectangular microstrip antenna,

$$\begin{bmatrix} J_\phi(\phi,\, z) \\ J_z(\phi,\, z) \end{bmatrix} = \frac{1}{2\pi}\sum_{n=-\infty}^{\infty} e^{jn\phi}\int_{-\infty}^{\infty} d\,k_z\, e^{jk_z z}\begin{bmatrix} \tilde{J}_{\phi n}(k_z) \\ \tilde{J}_{zn}(k_z) \end{bmatrix} = \begin{bmatrix} 0 \\ 0 \end{bmatrix} \tag{4}$$

where J_z and J_ϕ, respectively, are the surface current densities on the rectangular microstrip antenna obtained in the z and ϕ directions. The integral equations are then determined using a Galerkin's method of moments calculation. $\tilde{J}_{zn}$ and $\tilde{J}_{\phi n}$ are the patch surface current in densities in the nth basis function in z and ϕ directions, respectively. The tilde denotes the spectral amplitude or a Fourier transform. The elements in the $\overset{\cong}{X}$ matrix is a dyadic Green's function in the spectral domain and can be expressed as in [8]. Once E_z and H_z are known, the other expression for transverse fields in each sector can be found [8, 10]. Considering a few more specific simplifications, the E_z and H_z fields in the outermost sector in all cases can be given as

$$\begin{bmatrix} E_z \\ H_z \end{bmatrix} = \frac{1}{2\pi}\sum_{n=-\infty}^{\infty} e^{j\,n\,\phi}\int_{-\infty}^{\infty} dk_z e^{j\,k_z z}\frac{H_n^{(2)}(k_\rho \rho)}{H_n^{(2)}(k_\rho\, R_5)}\overset{\cong}{X}^{-1}\begin{bmatrix} \tilde{J}_{\phi n}(k_z) \\ \tilde{J}_{zn}(k_z) \end{bmatrix} \tag{5}$$

where $k_\rho^2 = \omega^2\mu_0\varepsilon_i - k_z^2$. Again considering the stationary- phase evaluation, the far-field components in spherical coordinates are written approximately as

$$\begin{bmatrix} E_\theta \\ E_\phi \end{bmatrix} = \frac{1}{\sin\theta}\begin{bmatrix} -1 & 0 \\ 0 & \eta_0 \end{bmatrix}\begin{bmatrix} E_z \\ H_z \end{bmatrix} = \frac{1}{\sin\theta}\begin{bmatrix} -1 & 0 \\ 0 & \eta_0 \end{bmatrix}\frac{e^{jk_0 r}}{\pi r}\sum_{n=-\infty}^{\infty}\frac{(-j)^{(n+1)}e^{jn\phi}}{H_n^{(2)}(k_0 R_5\sin\theta)}\overset{\cong}{X}^{-1}\begin{bmatrix} J_\phi \\ J_z \end{bmatrix} \tag{6}$$

where η_0 is the free space intrinsic impedance. From Eq. (6), the directive gain of the microstrip patch as a radiator can be calculated as

$$D(\theta,\phi) = \frac{4\pi\left(|E_\theta|^2 + |E_\phi|^2\right)}{\int_0^{2\pi}\int_0^{\pi}\left(|E_\theta|^2 + |E_\phi|^2\right)\sin\theta d\theta d\phi} \tag{7}$$

The maximum value of Eq. (7) is defined as rectangular microstrip antenna directivity [1]. Similarly, the other parametric values like gain, return loss, and bandwidth can be determined [4, 11].

3. MODEL DESCRIPTION

The microstrip antenna model is designed using the HFSS^{TM} simulation tool which resonates at frequency 3.5 GHz, shown in Figure 2. The antenna models consist of RT Duroid 5880 dielectric material with a thickness of 0.127 mm for substrate and 0.254 mm for superstrate. The theoretical values for antenna dimensions and parameters are calculated using MATLAB^{TM}, and model results are obtained with simulation tool [11, 12]. A typical antenna dimension is 28.52 mm × 33.86 mm with microstrip inset feed adjusted at a 50 ohm feed impedance matching condition as shown in Figure 2(a). The fabricated dielectric loaded antenna model is folded and installed on a cylindrical block of diameter 500 mm for experimental measurements. In the dual-element antenna model, the dimensions of each element are the same as those of the single element with inter-element spacing fixed at half wavelength as shown in Figure 2(b). The procedures of simulation and testing will remain common for both models. All

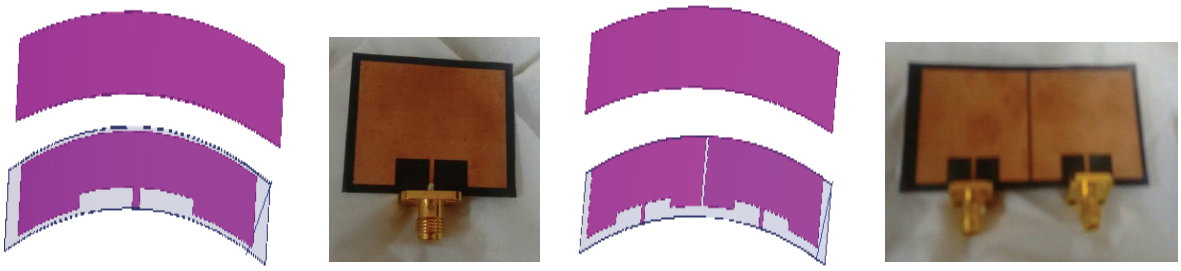

(a1) (a2) (b1) (b2)

Figure 2. (a) Single element antenna, (a1) model with air spaced superstrate, (a2) prototype patch antenna, (b) dual element antenna, (b1) model with air spaced superstrate, (b2) prototype patch antenna.

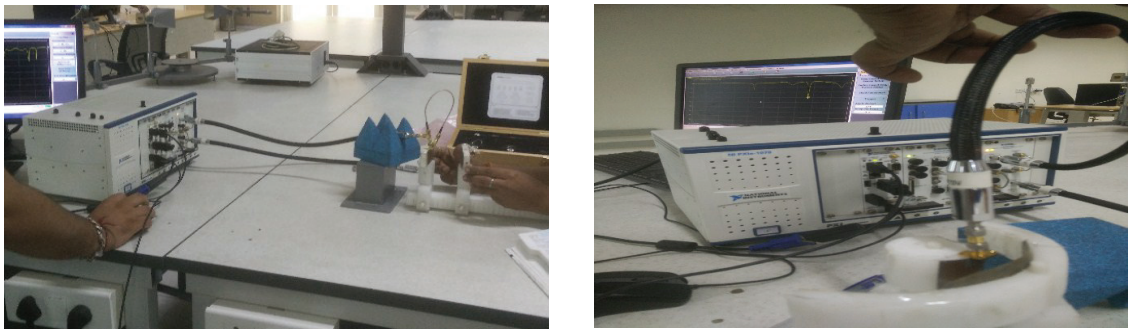

(a) (b)

Figure 3. Measurement setup for rectangular patch antenna model at different superstrate spacing.

the measurements are done by keeping the return loss below -10 dB with a VSWR range between 1 to 2. For performing the experiments, a customized test bench setup is developed which consists of two movable cylindrical carriage blocks for antenna and superstrate mounting. These blocks are able to slide along the length of a scaled rod at equal intervals and adjusted at particular position for testing as shown in Figure 3. For validation of the prototype antenna, this setup is very useful in performing the experiments more accurately and easily under the specified designed conditions.

4. OBSERVATIONS AND DISCUSSIONS

This paper has implemented the viability of a conformal cylindrical antenna under various dielectric loading separations. The simulated and measured results show the comparative antenna characteristics and are tabulated in Tables 1 and 2. The experiments have been performed on a conformal antenna by gradually varying the superstrate gap up to a quarter wavelength by keeping the curvature fixed and inter-element spacing at nearly half wavelength for the dual antenna model. The parametric observations of gain, directivity, and bandwidth for all these cases are plotted in Figures 4 and 5. These tables and figures show the curvature and loading effect on key parameters such as resonant frequency, bandwidth, directivity, and gain. Initially, the antenna measurement is taken without a superstrate, and a frequency shift due to bending is observed together with a nominal gain. When the superstrate is flush mounted on the patch ($S_p = 0$), there is a maximum effect of loading which shifts the resonant frequency towards the higher side of the band. Both the gain and directivity show an improvement in performance because of the increase in effective dielectric constant. Now, as the superstrate air gap starts increasing up to a quarter wavelength, the loading effect decreases, and therefore, the resonant frequency increases moderately [10]. A dielectric cover is used to enhance the gain of an aperture-coupled microstrip patch antenna. The cover is spaced off from the patch antenna by air, and it is found to significantly increase

Table 1. Parametric analysis of single rectangular patch antenna with varying superstrate air gap.

Fixed Diameter-500mm and $S_p = N\lambda/4$	Calculated Antenna Parameters					Measured Antenna Parameters				
	Resonant Freq. (GHz)	Return Loss (dB)	VSWR	Directivity (dB)	Gain (dB)	Resonant Freq. (GHz)	Return Loss (dB)	VSWR	Directivity (dB)	Gain (dB)
Without superstrate	6.8	-11.4	1.7	2.6	1.7	6.5	-11.1	1.6	2.4	1.4
N=0	6.5	-11.7	1.7	2.8	2.2	6.4	-10.20	1.8	2.5	2
N=0.25	6.4	-12.9	1.6	3.7	3.3	6.3	-12.4	1.7	3	2.6
N=0.5	6.4	-13.5	1.5	4	3.8	6.2	-12.7	1.6	3.4	3.1
N=0.75	6.4	-14.2	1.4	4.4	4.2	6.2	-13	1.5	3.9	3.3
N=1	6.4	-14.9	1.5	4.4	4.2	6.2	-12.9	1.7	4.3	4.1

Table 2. Parametric analysis of dual rectangular patch antenna with varying superstrate air gap at half wavelength inter-element spacing.

Fixed Diameter-500mm and $S_p = N\lambda/4$	Calculated Antenna Parameters					Measured Antenna Parameters				
	Resonant Freq. (GHz)	Return Loss (dB)	Mutual Coupling Coeff. (dB)	Directivity (dB)	Gain (dB)	Resonant Freq. (GHz)	Return Loss (dB)	Mutual Coupling Coeff. (dB)	Directivity (dB)	Gain (dB)
Without superstrate	7.7	-17.7	-29.8	4.3	2.8	7.5	-17.5	-28.9	4.1	1.6
N=0	7.4	-20.5	-28.7	4.6	2.2	7.1	-17.5	-25.6	4.4	2
N=0.25	7.4	-20.5	-28.7	4.7	3.5	7.1	-18.1	-26.3	4.5	3.2
N=0.5	7.4	-20.7	-28.7	4.8	3.9	7.1	-18.9	-27	4.5	3.5
N=0.75	7.4	-21	-28.8	4.9	4.2	7.2	-20.5	-27.6	4.8	3.9
N=1	7.5	-21.2	-29	5.2	4.7	7.3	-21	-28.4	5	4.2

the antenna broadside directivity. As a consequence, multiple reflections take place and give optimum at resonance condition which provides the maximum gain from 1.7 dB to 4.2 dB and 2.8 dB to 4.7 dB for single and dual antenna models at 500 mm diameter, respectively. At the same time, the enhancement in directivity is also observed up to 4.4 dB and 5.2 dB for the single and dual antenna models with a dielectric superstrate air gap of 0.25λ as compared to antenna without loading. The antenna gain and directivity variations plotted are a function of superstrate spacing as depicted in Figure 4. The

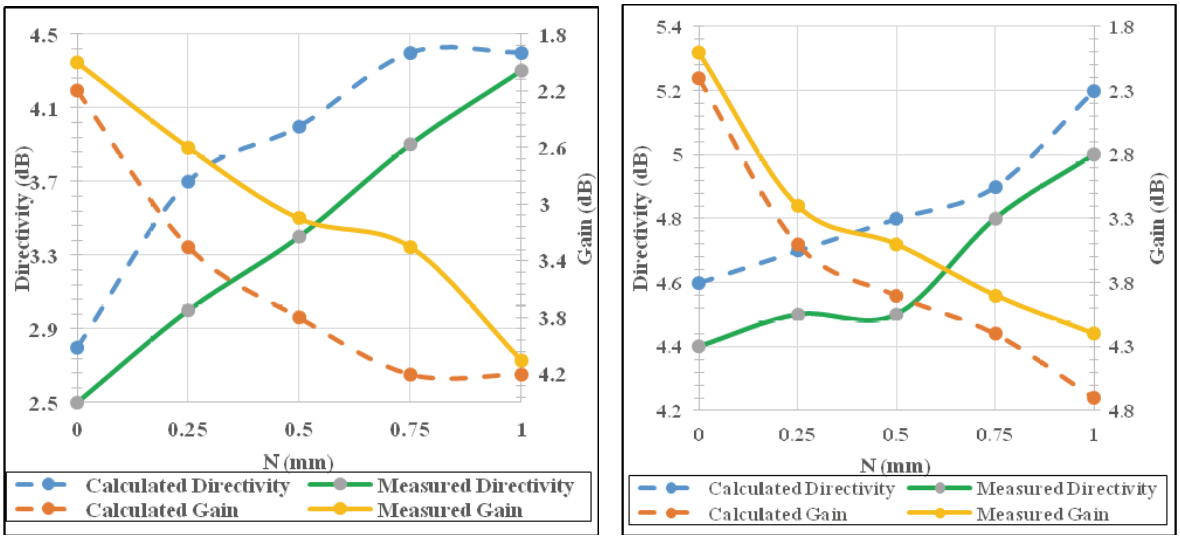

Figure 4. Gain and Directivity comparison plot w.r.t. varying superstrate air gap for (a) single cylindrical rectangular patch antenna. (b) Dual cylindrical rectangular patch antenna.

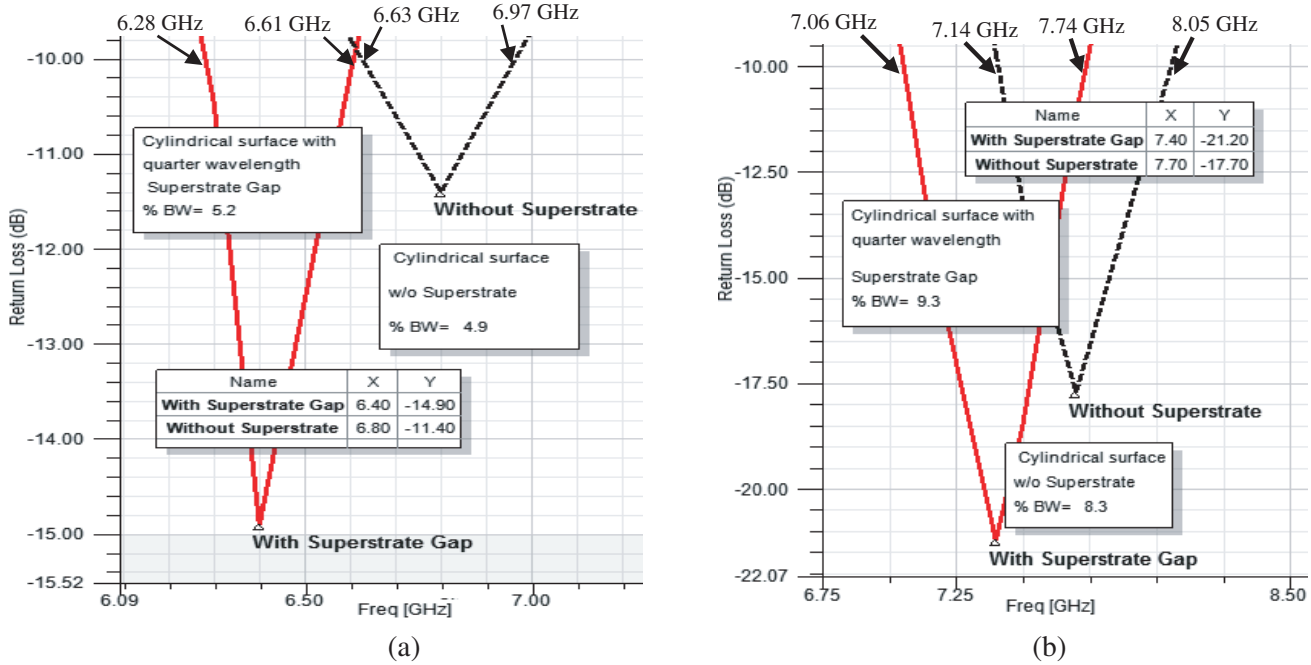

Figure 5. Bandwidth improvement plot as a function of without and with superstrate at air gap, $S_p = 0.25\lambda N$ at diameter = 500 mm for (a) single cylindrical rectangular patch antenna, (b) dual cylindrical rectangular patch antenna.

antenna gain and directivity have shown better results at $N = 1$ because of the resonance condition. Also, there is an improvement in input impedance bandwidth from 4.9% to 5.2% for the single antenna and 8.3% to 9.3% for the dual antenna as shown in Figure 5. This antenna parameter upgrading is due to the antenna's behaving as a directive parasitic antenna and becomes higher for the quarter spaced superstrate.

5. CONCLUSIONS AND FUTURE WORK

The analysis of antenna models with various superstrate positions is discussed and examined very thoroughly. The parametric study on the effects of spacing height of the cover is presented and validated. It is observed that an improvement of the antenna performance in terms of gain, directivity, and bandwidth is possible with efficient utilization of the superstrate which also provides protection. The impedance bandwidth of the dielectric loaded quarter wavelength gap antenna has increased up to 5.2% and 9.3% and directivity raised up to a level of 4.4 dB and 5.2 dB for single and dual antennas, respectively. By varying the antenna bending and superstrate spacing, the resonant frequency can also be shifted proportionally, allowing it to be used as a reconfigurable antenna. The recent advancement in the characteristics of the conformal antenna using metamaterials of with varying thicknesses and dielectric constants can be considered for future work.

REFERENCES

1. Wong, K. L., *Design of Nonplanar Microstrip Antennas and Transmission Lines*, 16–35, John Wiley & Sons, Inc., New York, 1999.
2. Singh, P. K. and J. Saini, "Effect of varying curvature and inter element spacing on dielectric coated conformal microstrip antenna array," *Progress In Electromagnetics Research M*, Vol. 58, 11–19, June 2017.
3. Bahl, I., P. Bhartia, and S. Stuchly, "Design of microstrip antennas covered with a dielectric layer," *IEEE Transactions on Antennas and Propagation*, Vol. 30, No. 2, 314–318, March 1982.
4. Singh, P. K. and J. Saini, "Reconfigurable microstrip antennas conformal to cylindrical surface," *Progress In Electromagnetics Research Letters*, Vol. 72, 119–126, January 2018.
5. Cooray, F. R. and J. S. Kot, "Analysis of radiation from a cylindrical rectangular microstrip patch antenna loaded with a superstrate and an air gap using the electric surface current model," *Progress In Electromagnetic Research*, Vol. 67, 135–152, 2007.
6. Meagher, C. J. and S. K. Sharma, "A wideband aperture-coupled microstrip patch antenna employing spaced dielectric cover for enhanced gain performance," *IEEE Transactions on Antennas and Propagation*, Vol. 58, No. 9, 314–318, September 1982.
7. Yang, H. Y. and N. G. Alexopoulos, "Gain enhancement methods for printed circuit antennas through multiple superstrates," *IEEE Transactions on Antennas and Propagation*, Vol. 35, No. 8, 860–863, July 1987.
8. Zaiki, A., N. A. M. Affendi, N. A. L. Alias, and N. M. Razali, "Flexible antennas based on natural rubber," *Progress In Electromagnetics Research C*, Vol. 61, 75–90, 2016.
9. Wong, K. L., Y. T. Cheng, and J. S. Row, "Resonance and radiation of a superstrate loaded cylindrical rectangular microstrip patch antenna with an air gap," *Proc. Natl. Sci. Count. ROC (A)*, Vol. 17, 365–371, September 1993.
10. Singh, P. K. and J. Saini, "Performance analysis of superstrate loaded cylindrically conformal microstrip antenna on the varying curvature for Wimax applications," *International Journal of Microwave and Optical Technology*, Vol. 11, No. 6, 406–412, November 2016.
11. Singh, P. K. and J. Saini, "Mutual coupling analysis of dielectric coated microstrip antennas mounted on the cylindrical surface with varying inter element spacing," *IEEE International Conference on Signal Processing and Communication*, No. 3, 100–105, December 2016.
12. Balanis, C. A., *Antenna Theory, Analysis and Design*, 3rd Edition, 811–876, John Wiley & sons, New York, 2005.